# Epe1 recruits BET family bromodomain protein Bdf2 to establish heterochromatin boundaries

**Jiyong Wang,[1] Xavier Tadeo,[1] Haitong Hou,[1] Patricia G. Tu,[2] James Thompson,[2] John R. Yates III,[2] and Songtao Jia[1,3]**

[1]Department of Biological Sciences, Columbia University, New York, New York 10027, USA; [2]Department of Chemical Physiology, The Scripps Research Institute, La Jolla, California 92037, USA

**Heterochromatin spreading leads to the silencing of genes within its path, and boundary elements have evolved to constrain such spreading. In fission yeast, heterochromatin at centromeres I and III is flanked by inverted repeats termed *IRC*s, which are required for proper boundary functions. However, the mechanisms by which *IRC*s prevent heterochromatin spreading are unknown. Here, we identified Bdf2, which is homologous to the mammalian bromodomain and extraterminal (BET) family double bromodomain proteins involved in diverse types of cancers, as a factor required for proper boundary function at *IRC*s. Bdf2 is enriched at *IRC*s through its interaction with the boundary protein Epe1. The bromodomains of Bdf2 recognize acetylated histone H4 tails and antagonize Sir2-mediated deacetylation of histone H4K16. Furthermore, abolishing H4K16 acetylation (H4K16ac) with an *H4K16R* mutation promotes heterochromatin spreading, and mimicking H4K16ac by an *H4K16Q* mutation blocks heterochromatin spreading at *IRC*s. Our results thus illustrate a mechanism of establishing chromosome boundaries at specific sites through the recruitment of a factor that protects euchromatic histone modifications. They also reveal a previously unappreciated function of H4K16ac in cooperation with H3K9 methylation to regulate heterochromatin spreading.**

[*Keywords*: BET; H4K16; acetylation; boundary; heterochromatin]

Supplemental material is available for this article.

Received April 30, 2013; revised version accepted August 8, 2013.

In eukaryotes, genomic DNA is folded with histone and nonhistone proteins in the form of chromatin. Chromatin regulates diverse DNA-based processes such as gene transcription, recombination, and DNA damage repair (Bannister and Kouzarides 2011; Zentner and Henikoff 2013). Based on the level of compaction, chromatin is categorized as euchromatin or heterochromatin. Euchromatin is gene-rich and usually associated with active transcription, whereas heterochromatin is gene-poor and highly compacted and limits the access of transcription and recombination machinery (Grewal and Jia 2007; Beisel and Paro 2011). Heterochromatin has the intrinsic ability to spread in a sequence-independent manner, inactivating genes over long distances (Talbert and Henikoff 2006; Grewal and Jia 2007; Moazed 2011). Thus, to maintain stable gene expression patterns, it is essential to protect euchromatin from encroachment by heterochromatin (Gaszner and Felsenfeld 2006; Valenzuela and Kamakaka 2006).

[3]**Corresponding author**
**E-mail jia@biology.columbia.edu**
Article is online at http://www.genesdev.org/cgi/doi/10.1101/gad.221010.113.

Heterochromatin spreading depends on the self-propagation of heterochromatin-associated histone modifications and chromatin proteins (Rusche et al. 2003; Talbert and Henikoff 2006; Moazed 2011). Histones within heterochromatin are methylated on H3 Lys9 (H3K9me), which serves as a signal for the recruitment of heterochromatin protein 1 (HP1) family proteins (Rea et al. 2000; Bannister et al. 2001; Nakayama et al. 2001). HP1 recruits the H3K9 methyltransferase SUV39 (Schotta et al. 2002; Stewart et al. 2005), leading to methylation of adjacent nucleosomes. This positive feedback loop induces heterochromatin spreading outwards from its nucleation sites (Talbert and Henikoff 2006). Histones within heterochromatin regions are also hypoacetylated. In budding yeast, which lacks H3K9me and HP1 proteins, the Sir2/Sir3/Sir4 complex mediates heterochromatin spreading in a similar fashion, where Sir2/Sir4-mediated deacetylation of histone H4K16 and recruitment of Sir3 form a similar self-propagating mechanism for heterochromatin spreading (Kurdistani and Grunstein 2003; Rusche et al. 2003; Moazed 2011). Given that H4K16 acetylation (H4K16ac) status directly affects the compaction levels of nucleosome arrays in vitro (Shogren-Knaak

et al. 2006), modulation of H4K16ac levels could potentially be a universal mechanism to regulate heterochromatin assembly and spreading. However, functional homologs of Sir3 and Sir4 are absent from organisms using H3K9me/HP1 systems to assemble heterochromatin, and the role of H4K16ac in regulating heterochromatin spreading outside of budding yeast is unknown.

Spreading of heterochromatin is limited by the availability of silencing proteins and competition between positive and negative regulatory components. As a result, the heterochromatin–euchromatin border is often not precisely defined but instead exhibits an extended transition zone (Kimura and Horikoshi 2004). In certain cases, heterochromatin is confined by specific DNA sequences termed boundary elements, which are characterized by sharp transitions in histone modification profiles (Gaszner and Felsenfeld 2006; Valenzuela and Kamakaka 2006). When the functions of such boundaries are disrupted, heterochromatin spreads and silences genes located outside of boundaries. Thus, boundary elements are essential for maintaining stable gene expression patterns. The mechanisms that specify heterochromatin boundaries are diverse, but most function by either recruiting histone-modifying enzymes to directly antagonize heterochromatin-associated histone modification cycles or tethering chromatin to the nuclear envelope to physically separate different chromatin domains (Gaszner and Felsenfeld 2006; Valenzuela and Kamakaka 2006).

Heterochromatin assembly has been extensively studied in fission yeast. Constitutive heterochromatin is mainly present at the pericentric, subtelomeric, and silent mating type regions of the fission yeast genome. All of these regions contain similar DNA elements that serve as nucleation centers of heterochromatin assembly through the RNAi pathway (Moazed 2009; Lejeune and Allshire 2011; Castel and Martienssen 2013). Additional DNA-binding proteins such as Atf1/Pcr1 and Taz1 promote heterochromatin nucleation within the silent mating type region and telomeres, respectively (Jia et al. 2004; Kanoh et al. 2005). These nucleation sites recruit the histone methyltransferase Clr4 complex (CLRC), leading to H3K9me and the recruitment of the HP1 homolog Swi6 (Nakayama et al. 2001; Hong et al. 2005; Horn et al. 2005; Jia et al. 2005). Once initiated, heterochromatin spreads from these nucleation centers into neighboring regions (Hall et al. 2002; Kanoh et al. 2005). The silent mating type and pericentric regions are surrounded by special DNA sequences that correspond to sharp transitions of histone modification profiles (Noma et al. 2001; Cam et al. 2005). At the mating type region, heterochromatin is flanked by two inverted repeats that recruit TFIIIC (Noma et al. 2006), the machinery required for RNA polymerase III (Pol III)-mediated transcription (Paule and White 2000). TFIIIC tethers its binding sites to the nuclear periphery, a process that may contribute to formation of heterochromatin boundaries (Noma et al. 2006). Some pericentric heterochromatin borders correlate with the presence of tRNA gene clusters (Cam et al. 2005), which are critical for boundary function (Scott et al. 2006). Given that Pol III transcribes tRNA genes, it is possible that these tRNA genes mediate boundary formation through a TFIIIC-based mechanism. There are also inverted repeats flanking centromeres I and III termed *IRC*s, which are also required for boundary activity (Noma et al. 2006), but the mechanism by which *IRC*s define heterochromatin boundaries is unknown.

Epe1 is a JmjC domain-containing protein required for boundary function (Ayoub et al. 2003). It is recruited to all heterochromatin domains in a Swi6-dependent manner (Zofall and Grewal 2006; Trewick et al. 2007; Sadaie et al. 2008) but is concentrated at borders of heterochromatin, such as *IRC*s, due to the degradation of Epe1 in the middle of heterochromatin by the proteasome, mediated by the Cul4–Ddb1 E3 ubiquitin ligase complex (Braun et al. 2011). Although JmjC domain proteins are generally involved in histone demethylation, Epe1 does not possess such activity (Tsukada et al. 2006), and the mechanism by which Epe1 functions in blocking heterochromatin spreading is still unknown.

By systematically screening a fission yeast deletion library for mutations that result in heterochromatin boundary defects, we identified a novel protein, Bdf2, required for heterochromatin boundary function at *IRC*s. Bdf2 interacts with Epe1 and is recruited to *IRC*s in an Epe1-dependent manner. Through its double bromodomains, Bdf2 preferentially interacts with acetylated histone H4 tails and protects them from Sir2-mediated deacetylation of H4K16. Our results demonstrate that protection of a euchromatic histone modification by a chromatin modification binding protein at a specific DNA element is sufficient to establish a heterochromatin boundary. We also uncovered a previously unappreciated role of H4K16ac in regulating heterochromatin spreading in a system where heterochromatic silencing is dominated by H3K9me and HP1.

## Results

### *IRC1 is a heterochromatin boundary*

The right border of pericentric heterochromatin on chromosome I corresponds to the presence of an *IRC* element (*IRC1R*). There are neither any tRNA genes nor any detectable TFIIIC enrichment (Noma et al. 2006), making it an ideal location to study *IRC* function. We inserted a *ura4*$^+$ reporter gene to the right of *IRC1R* (*IRC1R::ura4*$^+$) (Fig. 1A). Because heterochromatin spreading depends on the dosage of heterochromatin proteins, overexpression of Swi6 has been used to improve heterochromatin spreading at the silent mating type region and centromeres (Noma et al. 2001, 2006). Therefore, we inserted an additional copy of *swi6*$^+$ at the *ade6* locus to enhance heterochromatin spreading. In wild-type cells, *IRC1R::ura4*$^+$ was fully expressed, and cells could not grow on counterselective medium containing 5-fluoroorotic acid (FOA), which is toxic to cells expressing Ura4 (Fig. 1B). However, when *IRC1R* was deleted, the spreading of heterochromatin led to silencing of this reporter, as evidenced by increased growth on FOA medium (Fig. 1B). This silencing was eliminated in *clr4Δ* cells (Fig. 1B), suggesting that Clr4-mediated H3K9me is critical for heterochromatin spreading.

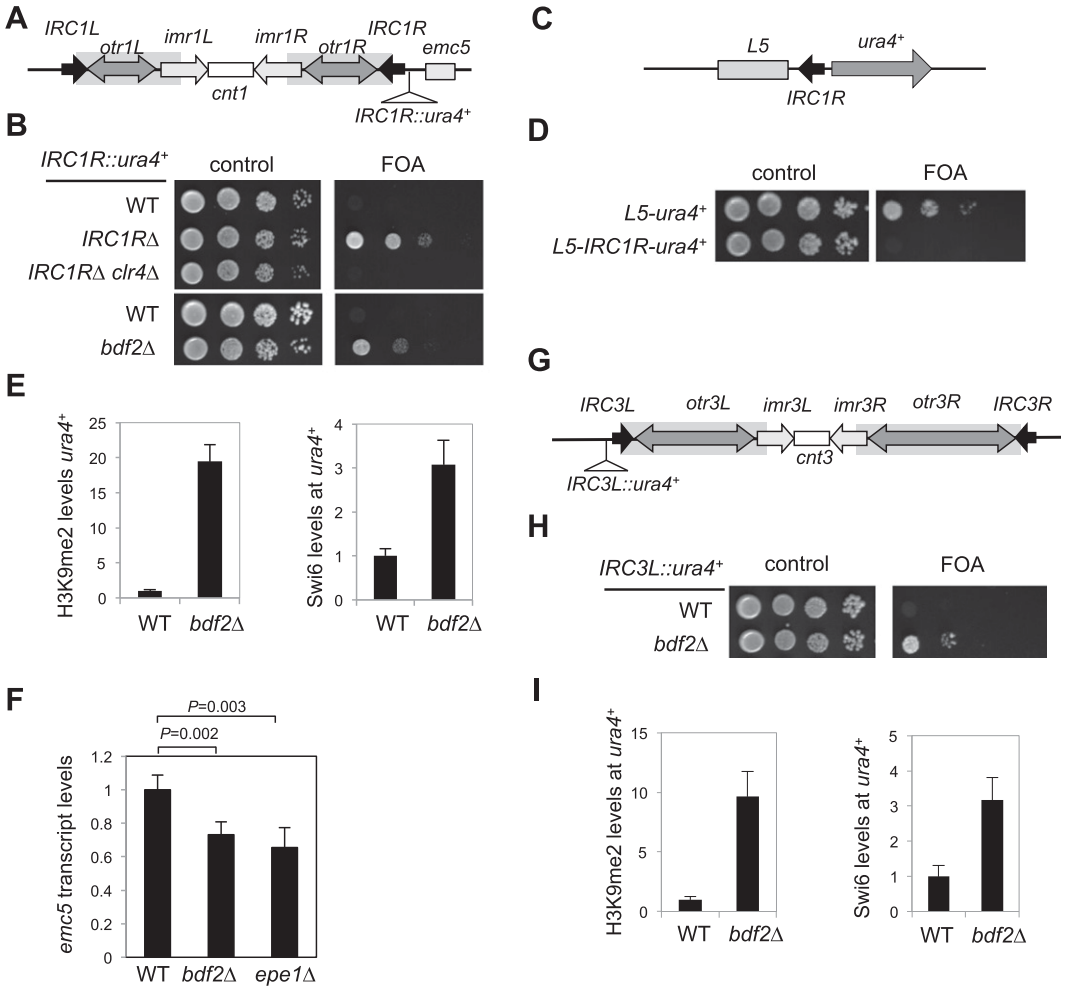


**Figure 1.** Bdf2 is required for boundary function. (*A*,*C*,*G*) Schematic diagrams of the *IRC1R::ura4*$^+$, *L5-IRC1R-ura4*$^+$, and *IRC3L::ura4*$^+$ reporters. (*B*,*D*,*H*) Tenfold serial dilution analyses of the indicated yeast strains were grown on the indicated medium to measure the spreading of heterochromatin into the *ura4*$^+$ reporter. (*E*,*I*) ChIP analysis of H3K9me2 and Swi6 levels at the *ura4*$^+$ reporters, normalized to *act1*. The data are averages of three experiments, and error bars represent standard deviation. (*F*) qRT–PCR analysis of *emc5* transcript levels, normalized to *act1*. Data presented are averages of three experiments, and error bars represent standard deviation.

Because the effect of *IRC1RΔ* on heterochromatin spreading might be a result of moving the *ura4*$^+$ reporter closer to heterochromatin, we also tested whether *IRC1R* is sufficient to block heterochromatin spreading. Ectopic insertion of a part of a pericentric repeat (*L5*) induces silencing of an adjacent *ura4*$^+$ reporter gene (Partridge et al. 2002; Sadaie et al. 2008). Interestingly, when we inserted *IRC1R* between *L5* and *ura4*$^+$ (Fig. 1C), heterochromatin spreading was blocked, as indicated by the failure of cells to grow on FOA medium (Fig. 1D). Thus, *IRC1R* is both necessary and sufficient for boundary function.

### *Bdf2 is required for proper boundary function*

To identify factors required for boundary function, we screened a fission yeast haploid deletion library containing ~3500 individual deletions of nonessential genes (Kim et al. 2010) for mutants that showed heterochromatin spreading (Supplemental Fig. S1). Our screen identified *epe1Δ*, which is known to be required for boundary function (Ayoub et al. 2003; Zofall and Grewal 2006; Trewick et al. 2007), as well as an uncharacterized null mutant of *SPAC631.02*, which has been named *bdf2*$^+$ (Garabedian et al. 2012) and *nrc1*$^+$ in PomBase. The Bdf2 protein contains two bromodomains and is homologous to the mammalian bromodomain and extraterminal (BET) family of double bromodomain proteins (Supplemental Fig. S2; Belkina and Denis 2012; Prinjha et al. 2012), which were recently identified as therapeutic targets for a number of cancers (Dawson et al. 2011; Zuber et al. 2011).

We confirmed that *bdf2Δ* resulted in heterochromatin spreading into *IRC1R::ura4*$^+$, as indicated by growth on FOA plates (Fig. 1B). Furthermore, heterochromatin hallmarks such as H3K9 dimethylation (H3K9me2) and Swi6 spread to the reporter gene, as indicated by chromatin immunoprecipitation (ChIP) analyses (Fig. 1E). Histone 3

levels at the reporter were unaffected by *bdf2Δ* (Supplemental Fig. S3A), indicating that the change in H3K9me2 levels was specific for this modification. Moreover, the expression level of *emc5*, which is the gene immediately adjacent to *IRC1R,* was reduced in *bdf2Δ* cells (Fig. 1F), suggesting that heterochromatin spreading regulates the expression of neighboring genes.

Similarly, *bdf2Δ* cells showed heterochromatin spreading into *ura4*$^+$ inserted outside of the centromere III heterochromatin boundary (*IRC3L::ura4*$^+$) (Fig. 1G–I) and the silent mating type region heterochromatin boundary (*IRR::ura4*$^+$) (Supplemental Fig. S4A,B; Singh and Klar 2008). Given that *IR*s and *IRC*s do not share sequence homology, our results indicate that Bdf2 is required for proper boundary functions at different locations, independent of the presence of *IRC*s.

### *Bdf2 is enriched at heterochromatin boundaries*

To examine the cellular functions of Bdf2, we generated a C-terminally Flag-tagged version of Bdf2 expressed from its endogenous chromosomal location. Bdf2-Flag was functional, as no defects in boundary function were observed (Supplemental Fig. S5A). We performed ChIP–chip analyses of Bdf2-Flag and H3K9me2 using an Agilent whole-genome microarray with additional customized probes that provide high coverage of centromeres. Bdf2 was enriched at all *IRC* elements, which correspond to sharp decreases in H3K9me2 levels (Fig. 2A,E). The localization of Bdf2 to *IRC*s was further confirmed by ChIP and quantitative real-time PCR (qPCR)-based analyses (Fig. 2B,F). Bdf2 also localized at the right border of centromere II heterochromatin, which correlates with a sharp drop of H3K9me2 levels but does not contain any *IRC* element (Fig. 2C,D). Interestingly, Bdf2 was not enriched at the left side of the centromere II heterochromatin boundary (Fig. 2C). We also found that Bdf2 localized at the mating type region boundary *IR*, although at lower levels compared with centromere boundaries (Supplemental Fig. S4C). Moreover, we found that Bdf2 also localized selectively at the promoter regions of a small group of genes (Supplemental Fig. S6A,B), indicating a possible role of Bdf2 in transcriptional regulation in addition to its role in boundary function.

### *Bdf2 interacts with Epe1*

To investigate further the function of Bdf2, we performed affinity purification of Bdf2-Flag and identified interacting proteins by mass spectrometry (Supplemental Fig. S7A; Supplemental Table S1). Significantly, among the proteins identified that specifically associated with Bdf2 but were absent in control purifications was the boundary protein Epe1 (Fig. 3A), consistent with Bdf2's boundary function. Bdf2 was also associated with a number of TAFs (TBP-associated factors) (Supplemental Fig. S7B), which might explain the promoter localization of Bdf2 in euchromatic regions. ChIP analyses of Taf10-Flag indicated that TAFs are not enriched at heterochromatin boundaries (Supplemental Fig. S7C). Conversely, affinity purification of Epe1-Flag also identified Bdf2 (Fig. 3A; Supplemental Table S1). To confirm the interaction between Bdf2 and Epe1, we performed coimmunoprecipitation analysis with extracts from cells expressing both Bdf2-myc and Epe1-Flag from their endogenous chromosomal loci. When Epe1-Flag was immunoprecipitated with anti-Flag-agarose resin, Bdf2 specifically copurified as well, demonstrating that Bdf2 interacts with Epe1 in vivo (Fig. 3B). Moreover, the interaction persisted when the cell lysates were treated with ethidium bromide (Fig. 3B), suggesting that the interaction between Epe1 and Bdf2 is direct rather than DNA-mediated.

Epistasis analysis showed that a *bdf2Δ epe1Δ* double mutant resulted in heterochromatin spreading similar to that of *epe1Δ*, suggesting that Bdf2 and Epe1 function in the same pathway (Fig. 3C). We also consistently observed that *epe1Δ* resulted in a slightly greater increase in heterochromatin spreading than *bdf2Δ*, suggesting additional roles for Epe1 in regulating boundary functions (Fig. 3C).

To examine the relationship between Bdf2 and Epe1, we performed ChIP analysis of Bdf2-Flag in an *epe1Δ* strain. Interestingly, Bdf2 localization at *IRC1* and *IRC3* was lost or significantly reduced in *epe1Δ* cells (Fig. 3D). Bdf2 protein levels and Bdf2 localization to the promoter of *oca8* were not affected by *epe1Δ* (Supplemental Figs. S6C, S8), indicating that Epe1 only regulates the localization of Bdf2 at *IRC*s. Epe1 is recruited to heterochromatin by Swi6 (Zofall and Grewal 2006; Trewick et al. 2007; Sadaie et al. 2008; Braun et al. 2011). As expected, Bdf2 was also delocalized from *IRC1* and *IRC3* in *swi6Δ* cells (Fig. 3D). On the other hand, the localization of Epe1 to *IRC*s was not affected by *bdf2Δ* (Fig. 3D). These results suggest that Epe1 functions upstream of Bdf2 for localization to *IRC*s.

We further demonstrated that Bdf2 and Epe1 interacted in a yeast two-hybrid assay (Fig. 3E,F), suggesting that the interaction between these two proteins might be direct. To determine the region of Bdf2 that mediates interaction with Epe1, we generated Bdf2 fragments that lack the N-terminal region (ΔN), the C-terminal region (ΔC), or both (BD) (Fig. 3E). We found that Bdf2 lacking the C-terminal region failed to interact with Epe1 in yeast two-hybrid assays (Fig. 3F). Moreover, coimmunoprecipitation showed that Bdf2-ΔC-myc interaction with Epe1-Flag was strongly reduced (Fig. 3G), suggesting that the C-terminal region of Bdf2 is required for Bdf2–Epe1 interaction in vivo. As expected, Bdf2-ΔC localization to *IRC1* was reduced (Fig. 3H), concomitant with heterochromatin spreading into *IRC1R::ura4*$^+$ (Fig. 3I).

### *The bromodomains of Bdf2 are required for boundary function*

Bromodomains are well known for their ability to bind acetylated lysines (Mujtaba et al. 2007). Bdf2 contains two bromodomains (Fig. 4A), but their binding specificities are unknown. Binding assays of recombinant GST-Bdf2-BD (amino acids 229–497, encompassing both bromodomains) with an array of histone tail peptides containing different combinations of post-translational modifications showed that Bdf2 preferentially binds to multiply acetylated histone H4 tail peptides (Supplemental Fig. S9).

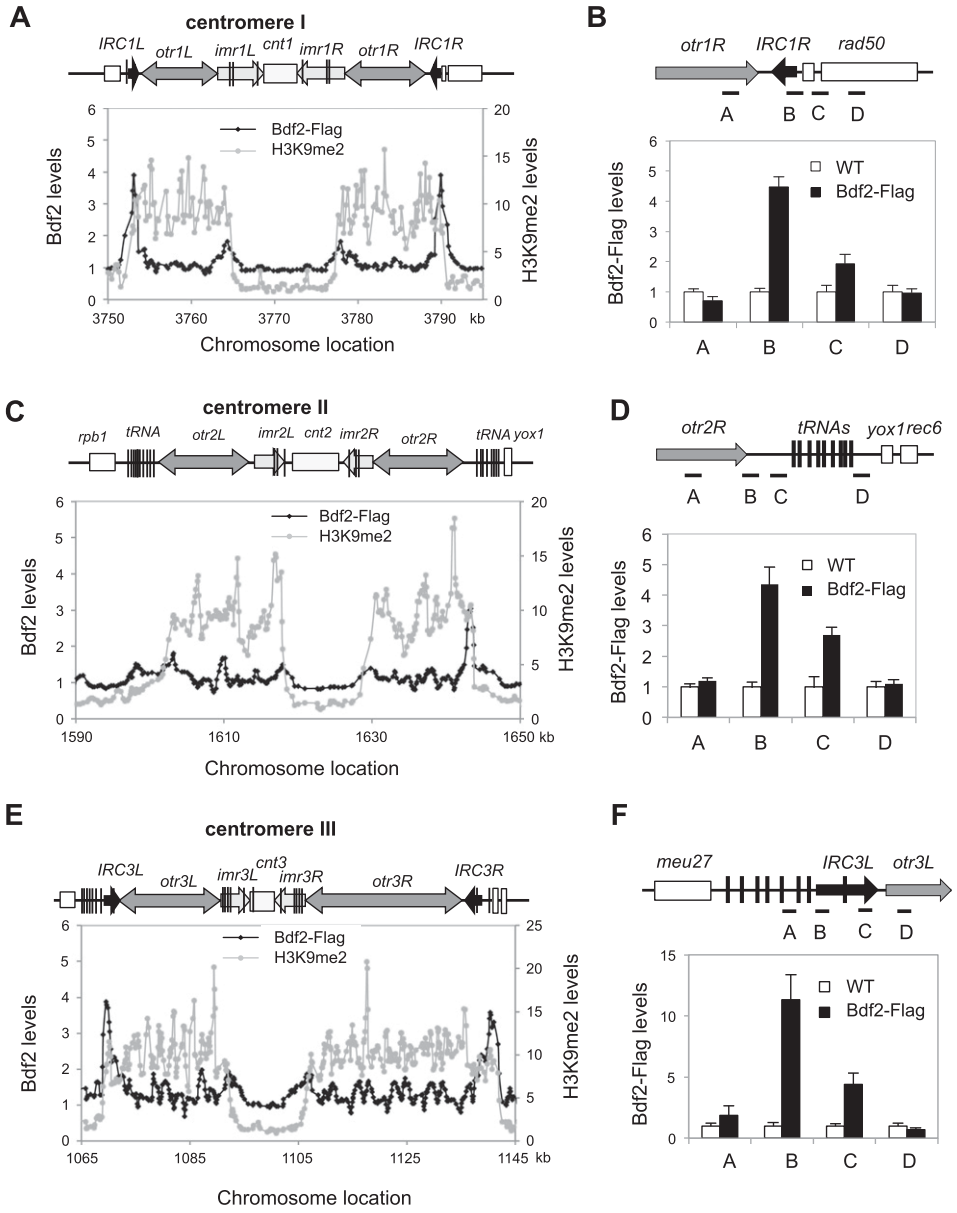


**Figure 2.** Bdf2 is enriched at *IRC*s. (*A*,*C*,*E*) ChIP–chip analysis of Bdf2-Flag and H3K9me2 levels across centromeres I, II, and III. The data are averages of two microarrays. Black arrows in the diagrams indicate the positions of *IRC*s. Bars indicate *tRNA* genes. Note that centromere II does not contain *IRC*s. (*B*,*D*,*F*) ChIP-qPCR analysis of Bdf2-Flag levels at boundary regions, normalized to *act1*. The positions of amplified regions used for qPCR quantification are indicated. The data are averages of three experiments, and error bars represent standard deviation.

Such results are consistent with those of a systematic study of BET family bromodomains, which indicates that they usually have broad specificity and preferentially bind to multiply acetylated histone tails (Filippakopoulos et al. 2012). To confirm this finding, we generated recombinant His-Bdf2-BD and examined its binding to a tetra-acetylated histone H4 tail peptide (K5, K8, K12, and K16) and a diacetylated histone H3 peptide (K9 and K14). Bdf2-BD bound strongly to the acetylated H4 peptide but not to its unacetylated form (Fig. 4B). Moreover, mutations of two amino acids that are predicted to form acetyl-lysine-binding sites, one in each of the bromodomains (Y268A and Y430A, hereafter denoted as 2YA) (Supplemental Fig. S2; Mujtaba et al. 2007), abolished this binding, indicating that Bdf2 binds to acetylated histone tails through its bromodomains (Fig. 4B). Bdf2 had little affinity for the diacetylated histone H3 peptide or any of the singly acetylated H4 peptides (Fig. 4B; data not shown), so it seems to prefer multiply acetylated H4 tails.

To examine further the role of bromodomains of Bdf2 in boundary function, we introduced the 2YA mutations at the endogenous *bdf2*$^+$ chromosomal location. Interestingly, boundary function was compromised to a degree similar to that of *bdf2Δ*, as indicated by silencing of

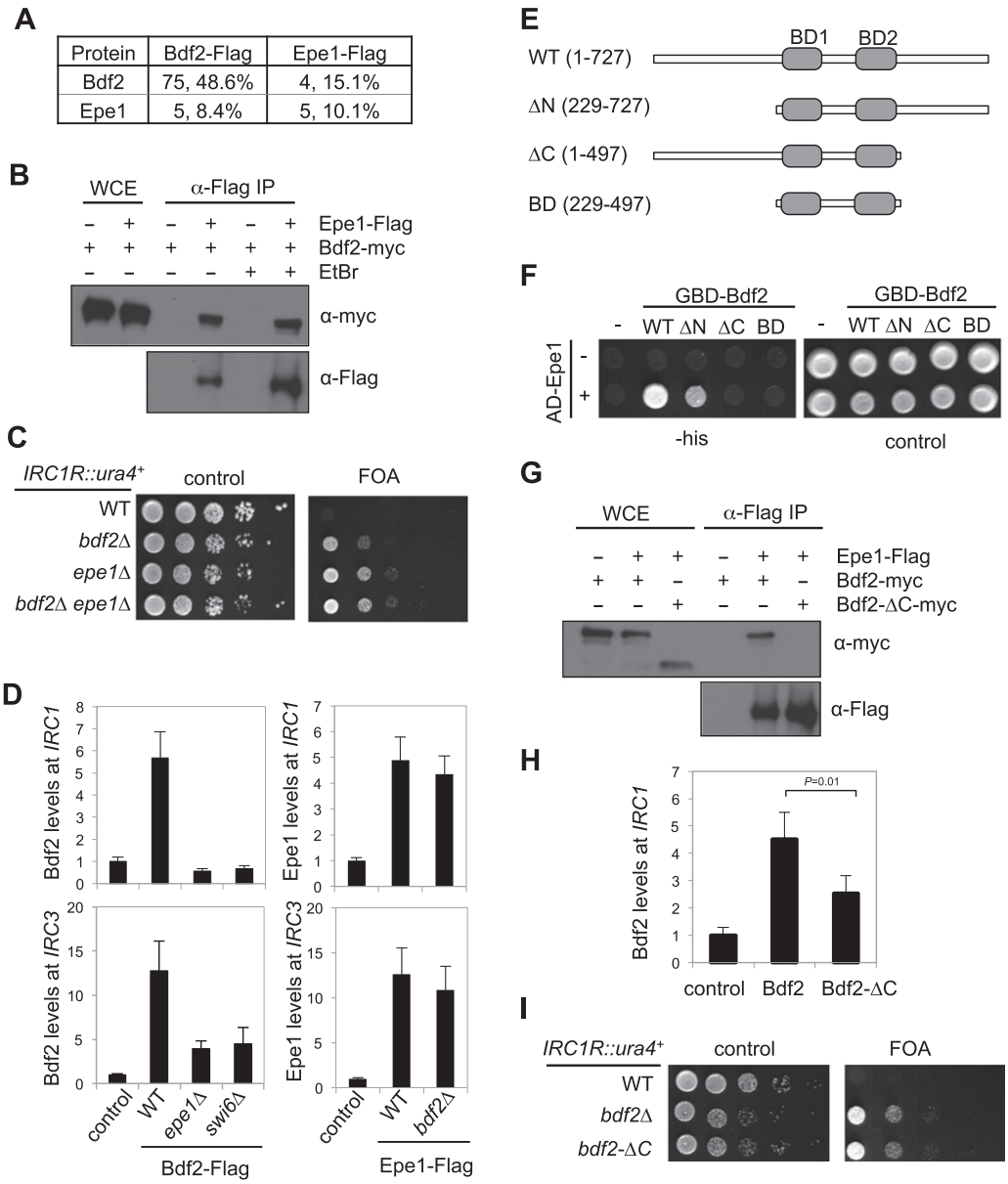


**Figure 3.** Epe1 recruits Bdf2 to *IRC*s. (*A*) Multidimensional protein identification technology (MudPIT) mass spectrometry analyses of purified Bdf2-Flag and Epe1-Flag complexes. The number of Bdf2 and Epe1 peptides identified and the percentage of each protein that these peptides cover are indicated. (*B*,*G*) Cell extracts from the indicated strains were incubated with Flag-agarose beads to isolate Epe1-Flag. Bound proteins were resolved by SDS-PAGE, and Western blot analyses were performed with Myc and Flag antibodies. (*C*,*I*) Serial dilution analyses were performed to measure heterochromatin spreading outside of *IRC1R::ura4*$^+$. (*D*,*H*) ChIP analysis of Bdf2-Flag and Epe1-Flag levels at *IRC*s, normalized to *act1*. The data are averages of three experiments, and error bars represent standard deviation. (*E*) Diagram of Bdf2 constructs used in yeast two-hybrid analysis. (*F*) Yeast two-hybrid analysis of Bdf2 with Epe1. Bdf2 was fused with the Gal4 DNA-binding domain, and Epe1 was fused with an activation domain. Interaction between Bdf2 and Epe1 resulted in the activation of a *HIS3* reporter gene, allowing cells to grow in the absence of histidine.

*IRC1R::ura4*$^+$ (Fig. 4C) and the spreading of H3K9me2 and Swi6 into the reporter gene (Fig. 4D). These results suggest that binding of acetylated histone H4 tails by Bdf2 is critical for boundary function. The mutations had no effect on Bdf2 protein levels (Fig. 4F), and Bdf2 still localized at *IRC*s, although at lower levels compared with that of wild type (Fig. 4E). This result suggests that binding of Bdf2 to acetylated histones also stabilizes Bdf2 at *IRC*s. Neither the *Y268A* nor the *Y430A* single mutant affected heterochromatin boundary function (Supplemental Fig. S5B), suggesting that the two bromodomains have redundant roles, at least in regulating boundary formation at *IRC*s.

### *Tethering Bdf2 to DNA is sufficient to establish a heterochromatin boundary*

We further tested whether recruiting Bdf2 was sufficient to establish a heterochromatin boundary independent of

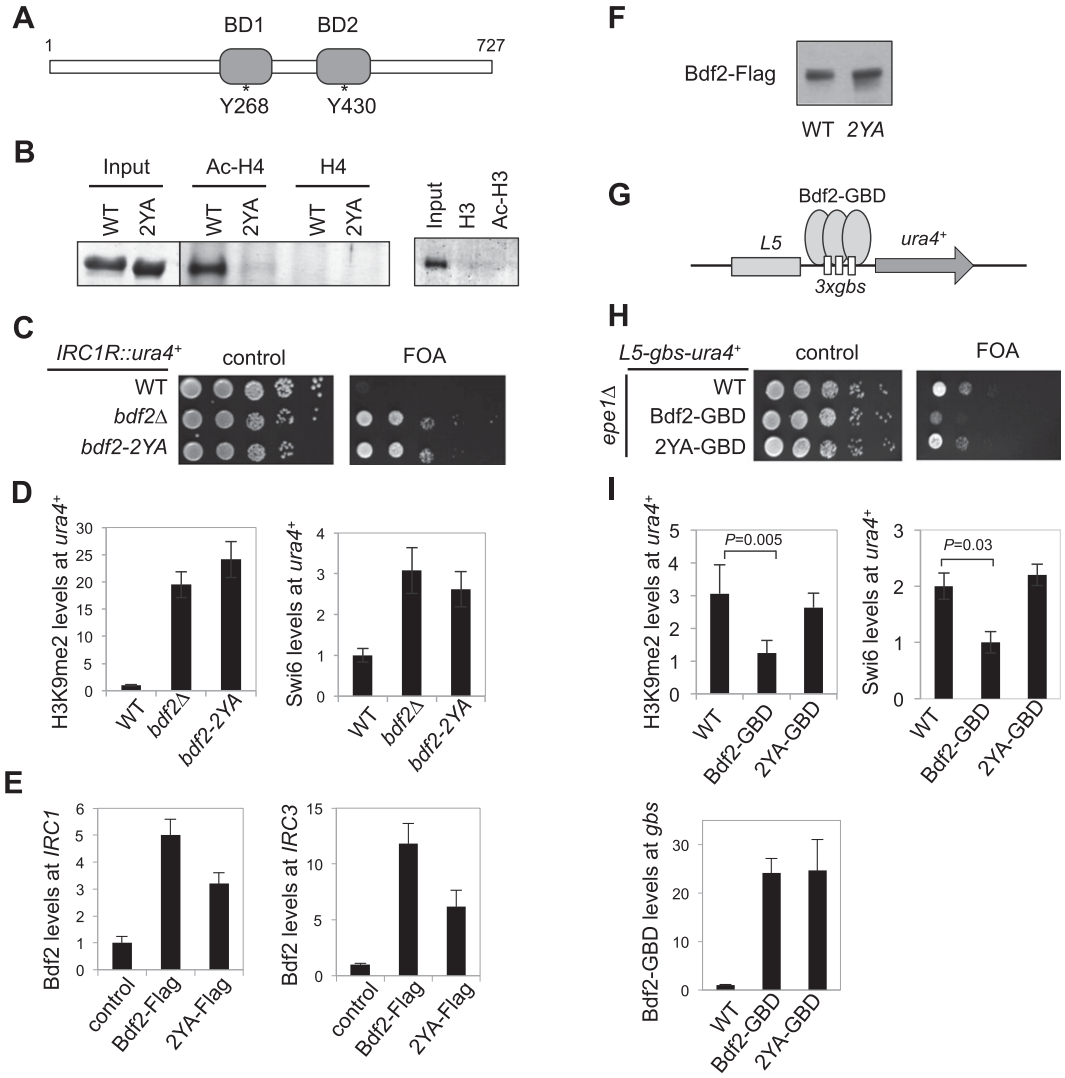


**Figure 4.** The bromodomains of Bdf2 are required for boundary function. (*A*) Schematic diagram of Bdf2 protein. The positions of mutations are indicated. (*B*) Peptide pull-down assays of the indicated recombinant proteins with biotinylated H4 tail (2–24) unmodified and tetra-acetylated at the K5, K8, K12, and K16 (Ac-H4) peptides as well as H3 tail (1–21) unmodified and diacetylated at the K9 and K14 (Ac-H3) peptides. (*C*) Serial dilution analysis to measure heterochromatin spreading outside of *IRC1R*::*ura4*$^+$. (*D*,*E*) ChIP analysis of H3K9me2 and Swi6 levels at *IRC1R*::*ura4*$^+$ and Bdf2-Flag levels at *IRC1R* and *IRC3L*, normalized to *act1*. The data are averages of three experiments, and error bars represent standard deviation. (*F*) Western blot analysis of Bdf2-Flag levels. (*G*) Schematic diagram of the *L5-gbs-ura4*$^+$ reporter. (*H*) Serial dilution analysis to measure heterochromatin spreading to *ura4*$^+$. All strains used contain *epe1Δ* to rule out the possibility that Bdf2 recruits Epe1 to establish heterochromatin boundaries. (*I*) ChIP analysis of H3K9me2 and Swi6 levels at *L5-gbs-ura4*$^+$ and Bdf2-GBD levels at *3xgbs*, normalized to *act1*. The data are averages of three experiments, and error bars represent standard deviation. All strains used contain *epe1Δ*.

Epe1. We inserted three copies of the Gal4-binding site (*gbs*) between *L5* and *ura4*$^+$ to create the *L5-gbs-ura4*$^+$ reporter (Fig. 4G). In the absence of Epe1, Bdf2-GBD, but not Bdf2-2YA-GBD, was able to block the spreading of heterochromatin from *L5* to *ura4*$^+$, as indicated by silencing assays (Fig. 4H) and ChIP analyses of H3K9me2 and Swi6 (Fig. 4I). Bdf2-GBD and Bdf2-2YA-GBD were equally enriched at *gbs* (Fig. 4I), indicating that it is not the binding of Bdf2 per se but rather its ability to bind acetylated histone H4 tails that is essential for boundary activity.

### *Bdf2 counteracts Sir2-mediated histone deacetylation*

The spreading of heterochromatin from nucleation sites depends on not only Clr4-mediated H3K9me and binding of Swi6, but also Sir2-mediated histone deacetylation (Hall et al. 2002; Shankaranarayana et al. 2003; Zhang et al. 2008; Buscaino et al. 2013;). However, *sir2Δ* has only minor effects on silencing of reporter genes inserted at pericentric heterochromatin (Shankaranarayana et al. 2003; Freeman-Cook et al. 2005; Alper et al. 2013; Buscaino et al. 2013), and it is not known whether Sir2 is required for

heterochromatin spreading outside *IRC*s. We generated *bdf2Δ sir2Δ* and *epe1Δ sir2Δ* strains with the *IRC1R::ura4*$^+$ reporter. In both cases, heterochromatin failed to spread to the reporter gene, as indicated by silencing assays and ChIP analyses (Fig. 5A–D), suggesting that heterochromatin spreading outside of its boundaries depends on Sir2.

### *The role of H4K16ac in regulating heterochromatin spreading*

The major substrates of Sir2 are H3K9ac and H4K16ac in vitro (Shankaranarayana et al. 2003; Alper et al. 2013). Since Clr4-mediated H3K9me is critical for heterochromatin assembly (Rea et al. 2000; Nakayama et al. 2001), it is conceivable that Sir2 functions to generate deacetylated H3K9 for subsequent action by Clr4. However, whether deacetylation of H4K16 is also involved in heterochromatin spreading is unknown. The fact that Bdf2 and Epe1 counteract Sir2 for boundary function and that Bdf2 binds to acetylated histone H4 instead of H3 tail suggests that H4K16ac also plays a role in regulating heterochromatin spreading. Indeed, ChIP analysis showed that H4K16ac levels at *IRC1* were significantly reduced in *epe1Δ* and *bdf2Δ* cells (Fig. 5E). Moreover, H4K16ac levels were increased in *sir2Δ* cells but restored to near wild-type levels in *epe1Δ sir2Δ* and *bdf2Δ sir2Δ* cells (Fig. 5E). Furthermore, recombinant Sir2 showed robust activity in an in vitro histone deacetylase (HDAC) assay when a tetra-acetylated histone H4 peptide was used as substrate, and this activity was strongly reduced when recombinant Bdf2, but not Bdf2-2YA, was added to the reaction (Fig. 5F).

If the function of Bdf2 is to protect H4K16ac, we expect that H4K16ac levels will be higher at heterochromatin boundaries where Bdf2 is present. To test this idea, we performed ChIP–chip analyses of H4K16ac at heterochromatin regions. H4K16ac levels were low in the middle of heterochromatin, which is consistent with the fact that heterochromatin is generally devoid of histone acetylation. Interestingly, however, H4K16ac levels spiked at heterochromatin boundaries, corresponding to Bdf2 peaks (Fig. 6A–C).

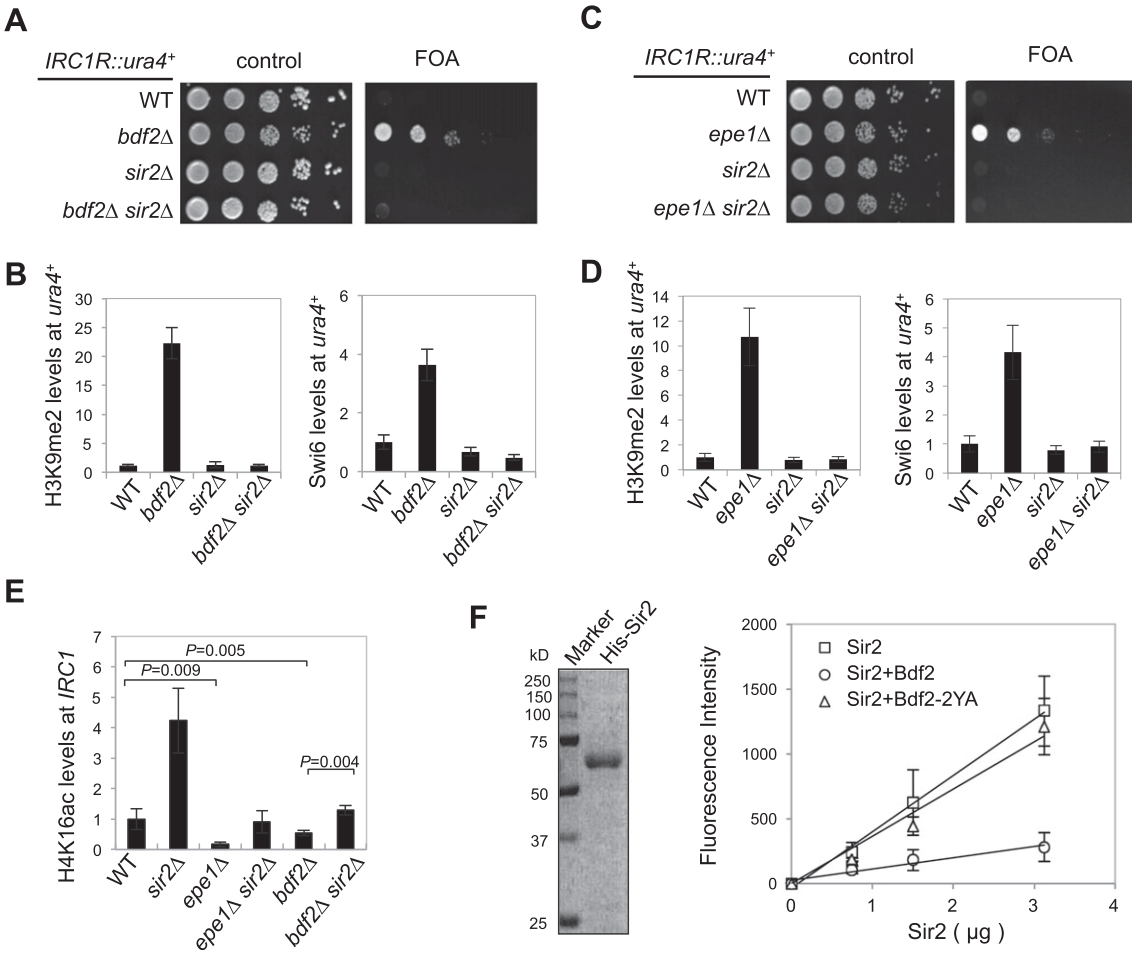


**Figure 5.** Bdf2 counteracts Sir2-mediated histone deacetylation. (*A*,*C*) Serial dilution analysis to measure heterochromatin spreading outside of *IRC1R::ura4*$^+$. (*B*,*D*,*E*) ChIP analysis of H3K9me2 and Swi6 levels at *IRC1R::ura4*$^+$ and H4K16ac levels at *IRC1*, normalized to *act1*. The data are averages of three experiments, and error bars represent standard deviation. (*F*, *left*) Coomassie-stained gel of recombinant Sir2. (*Right*) HDAC assays were performed with recombinant Sir2, a tetra-acetylated histone H4 peptide, and recombinant Bdf2. The production of nicotinamide was measured via the generation of nicotinic acid and free ammonia by nicotinamidase.

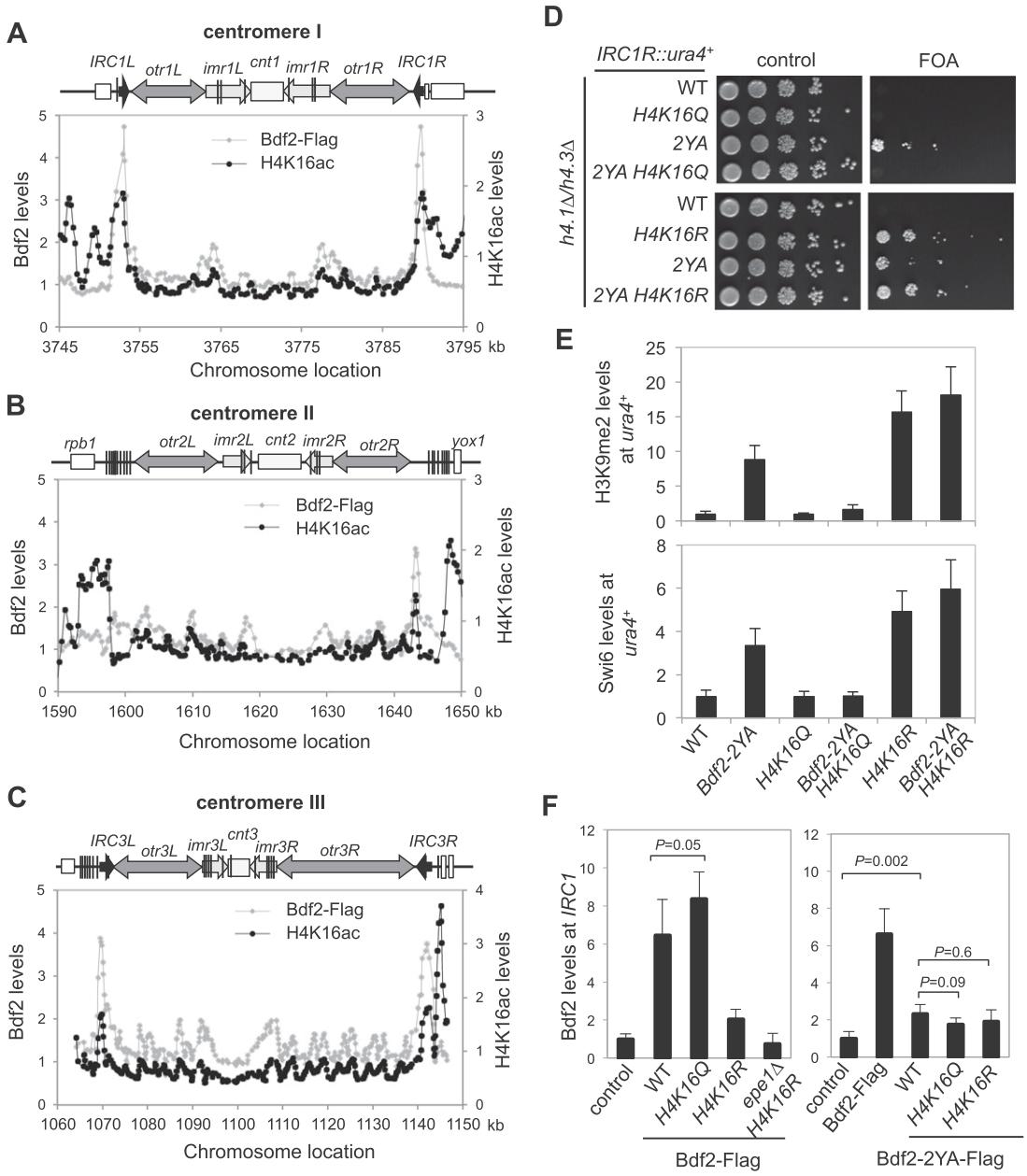


**Figure 6.** H4K16ac modulates heterochromatin boundary function. (*A–C*) ChIP–chip analysis of H4K16ac levels across centromeres I, II, and III. The Bdf2-Flag profile is also shown for comparison. (*D*) Serial dilution analysis to measure heterochromatin spreading outside of *IRC1R::ura4*$^+$. All strains used are in an *h4.1Δ/h4.3Δ* background. (*E,F*) ChIP analysis of H3K9me2 and Swi6 levels at *IRC1R::ura4*$^+$ and Bdf2 levels at *IRC1*, normalized to *act1*. The data are averages of three experiments, and error bars represent standard deviation. All strains used are in an *h4.1Δ/h4.3Δ* background.

To test directly whether deacetylation of H4K16 is required for heterochromatin spreading in fission yeast, we generated an *H4K16Q* mutation, which mimics H4K16ac. Fission yeast contains three pairs of H3/H4 genes, and deleting two of the H3/H4 pairs (*h4.1Δ/h4.3Δ*) allows the production of histone H4 from the remaining single copy (Mellone et al. 2003). In this background, histone H4 levels were reduced, as indicated by Western blot analyses (Supplemental Fig. S10A). Heterochromatin still spread into *IRC1R::ura4*$^+$ in *epe1Δ* cells albeit at lower efficiency, indicating that histone dosage also contributes to heterochromatin spreading (Supplemental Fig. S10B). Interestingly, in *bdf2-2YA H4K16Q* cells, heterochromatin failed to spread into *IRC1R::ura4*$^+$, as indicated by serial dilution analyses and ChIP analyses of H3K9me2 and Swi6 (Fig. 6D,E), suggesting that deacetylation of H4K16 is indeed required for heterochromatin spreading. Moreover, a *H4K16R* mutation, which abolished H4K16ac, resulted in heterochromatin spreading into *IRC1R::ura4*$^+$ (Fig. 6D,E). Similar results were obtained with *epe1Δ* and *bdf2Δ*

(Supplemental Fig. S11). The localization of Bdf2 to *IRC1* was reduced in *H4K16R* cells but slightly increased in H4K16Q cells (Fig. 6F). In contrast, the localization of Bdf2-2YA to *IRC1* was little affected by H4K16 mutations (Fig. 6F). These results demonstrate that Bdf2 is critical for regulating H4K16ac levels at boundaries and heterochromatin spreading.

### *Mst1 regulates H4K16ac levels at IRCs*

Among the histone acetyltransferases (HATs) in fission yeast, Mst1 is a member of the highly conserved MYST family of HATs, and it forms a complex similar to the NuA4 complex of budding yeast (Gomez et al. 2005, 2008; Shevchenko et al. 2008), which acetylates H4K16 (Lee and Workman 2007). We found that a *mst1-1* allele, which contains a temperature-sensitive *L344S* mutation (Gomez et al. 2008), resulted in heterochromatin spreading past *IRC1R* even at a permissive temperature, as indicated by the silencing of *IRC1R::ura4*$^+$ and the accumulation of H3K9me2 and Swi6 at the reporter (Fig. 7A,B). Moreover, in *mst1-1 H4K16Q* cells, heterochromatin spreading is abolished (Fig. 7A,B). Furthermore, *mst1-1* resulted in a significant decrease of H4K16ac levels and reduced recruitment of Bdf2 at *IRC1* (Fig. 7C,D). Thus, Mst1 directly regulates H4K16ac levels and the recruitment of Bdf2 at *IRC*s for proper boundary formation.

## Discussion

Proper formation of boundaries between chromosomal domains is essential for maintaining stable gene expression patterns (Gaszner and Felsenfeld 2006; Valenzuela and Kamakaka 2006). Here we showed that a double bromodomain protein of the BET family, Bdf2, is both necessary and sufficient for the formation of boundaries that limit the spreading of heterochromatin. We further showed that the bromodomains of Bdf2, which preferentially bind to multiply acetylated histone H4 tails, are critical for Bdf2 boundary function. Moreover, we demonstrated that Bdf2 directly protects histones from Sir2-mediated deacetylation and that the deacetylation of H4K16 is necessary for H3K9me and Swi6-mediated heterochromatin spreading. Below, we discuss the implications of our findings for heterochromatin spreading and boundary functions.

### *The role of Bdf2 in boundary formation*

The formation of heterochromatin has long been regarded as a paradigm for the assembly of self-propagating chromatin structures (Moazed 2011). The mechanism of heterochromatin spreading is complex and not well understood (Talbert and Henikoff 2006). A simplified view is that heterochromatin spreads by a positive feedback loop of histone modification and chromatin protein binding, the reiteration of which leads to the spreading of these modifications/proteins from nucleation sites (Talbert and Henikoff 2006; Grewal and Elgin 2007). There are two ways heterochromatin spreading is curbed. One is through competition between positive and negative forces, which

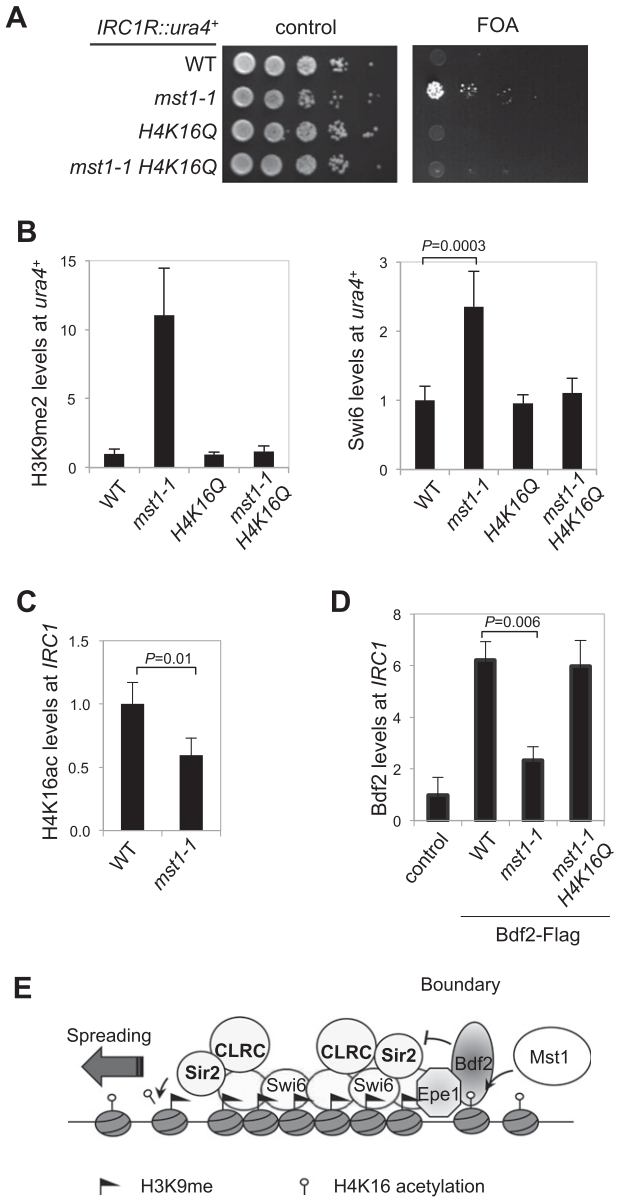


**Figure 7.** (*A*) Serial dilution analysis to measure heterochromatin spreading outside of *IRC1R::ura4*$^+$. All strains used are in an *h4.1Δ/h4.3Δ* background. (*B–D*) ChIP analysis of H3K9me2 and Swi6 levels at *IRC1R::ura4*$^+$ and H4K16ac and Bdf2 levels at *IRC1*, normalized to *act1*. The data are averages of three experiments, and error bars represent standard deviation. (*E*) A model by which H4K16ac and Bdf2 regulate heterochromatin spreading and boundary function. Heterochromatin spreading is mediated by cycles of Clr4-mediated H3K9me and the recruitment of Swi6. Sir2 mediates the deacetylation of H3K9, which is required for creating the substrate for Clr4, as well as the deacetylation of H4K16, which facilitates nucleosome compaction to bring the adjacent nucleosome closer to Clr4. Bdf2 is recruited to *IRC*s through Epe1, which is highly enriched at *IRC*s. Mst1 mediates H4K16ac at *IRC*s, which further stabilizes binding of Bdf2 to *IRC*s through its bromodomains. Bdf2 protects H4 tails from deacetylation by Sir2, preventing further heterochromatin spreading.

results in the formation of extended transition zones that fluctuate when the heterochromatin–euchromatin balance changes (Kimura and Horikoshi 2004). These borders are termed "negotiable borders," since they are not defined by DNA sequence but move depending on the dosage of opposing activities. For example, in the classical example of position effect variegation (PEV) in *Drosophila*, where the *white* gene is juxtaposed to pericentric heterochromatin due to chromosome rearrangement, it is stochastically silenced by heterochromatin in a portion of cells due to variegation in the distance of heterochromatin spreading, resulting in mottled eyes (Elgin and Reuter 2007). Most of the genes identified that affect PEV are involved in regulating chromatin function in general rather than boundary functions specifically (Elgin and Reuter 2007). The more reliable way to stop heterochromatin from spreading is by specific DNA elements that actively establish borders to stop the spreading of heterochromatin (Gaszner and Felsenfeld 2006; Valenzuela and Kamakaka 2006). These DNA elements recruit histone-modifying enzymes to directly modify histones to counteract heterochromatin spreading (Oki et al. 2004; West et al. 2004). Alternatively, they tether chromosomal regions to the nuclear periphery, resulting in physical separation of chromosomal domains (Ishii et al. 2002; Noma et al. 2006). Regardless of mechanism, the key to boundary formation is to break up the self-propagation of heterochromatic histone modifications. We showed here that Bdf2 disrupts this chain reaction by protecting modified histone tails from heterochromatic modifications through the recruitment of a histone tail-binding protein to the boundary region (Fig. 7E).

Bdf2 is recruited to *IRC*s through boundary protein Epe1 (Fig. 3D). This recruitment is dependent on the C-terminal region of Bdf2, which mediates its interaction with Epe1 (Fig. 3F–H). Loss of Epe1 resulted in the delocalization of Bdf2 from *IRC*s without affecting the localization of Bdf2 to gene promoters elsewhere in the genome (Fig. 3D; Supplemental Fig. S6C). However, Epe1 exhibits a broad localization pattern across entire heterochromatin domains, although Epe1 levels at *IRC* elements are higher compared with those in the middle of heterochromatin (Zofall and Grewal 2006; Braun et al. 2011). This suggests that high concentrations of Epe1 are required for Bdf2 localization to *IRC*s. Alternatively, other factors present at *IRC*s might enhance the interaction between Epe1 and Bdf2 to promote the localization of Bdf2 to *IRC*s. We favor the latter idea because even in *ddb1Δ* cells, which exhibit a significant increase of Epe1 at the body of heterochromatin, there is only marginal enrichment of Bdf2 at the heterochromatic repeats (Supplemental Fig. S12). It is possible that acetylated histone H4 stabilizes Bdf2 binding to chromatin, as indicated by lower levels of Bdf2 at *IRC*s when the bromodomains are compromised or when H4K16ac levels are reduced (Figs. 4E, 6F, 7D). The lack of Bdf2 enrichment at pericentric repeats in *ddb1Δ* cells is also consistent with this idea, since histones within heterochromatin regions are generally hypoacetylated (Kurdistani and Grunstein 2003; Grewal and Elgin 2007). The localization of Bdf2 at the right side of the centromere II heterochromatin boundary (Fig. 2B,E), which does not show elevated Epe1 levels (Zofall and Grewal 2006), is also consistent with the idea that additional mechanisms contribute to Bdf2 recruitment to heterochromatin boundaries. The high concentration of Epe1 at heterochromatin boundaries is achieved through Cul4–Ddb1-mediated degradation of Epe1 in the middle of heterochromatin (Braun et al. 2011) and thus should be independent of DNA sequences. However, heterochromatin borders at centromeres and the silencing mating type region are well defined, suggesting that boundary DNA elements have independent contributions to shape the localization of Epe1 and Bdf2.

Overexpression of Epe1 results in defects in pericentric heterochromatin assembly (Zofall and Grewal 2006; Trewick et al. 2007) even in *bdf2Δ* cells (Supplemental Fig. S13), suggesting that Epe1 negatively regulates heterochromatin assembly independently of its role in recruiting Bdf2. Such an activity may also contribute to the boundary function of Epe1. This idea is further supported by the fact that *epe1Δ* showed stronger spreading of heterochromatin than *bdf2Δ*. Although Epe1 has also been proposed to be a demethylase or a hydroxylase and mutations of putative active site residues affect Epe1 function (Trewick et al. 2005, 2007), the substrate of Epe1 has not been identified. Further characterization of the enzymatic activity of Epe1 is needed to reveal additional mechanisms by which Epe1 regulates heterochromatin spreading.

In budding yeast, the double bromodomain protein Bdf1 is also required to prevent Sir2-mediated heterochromatin spreading near telomeres through the binding of Bdf1 to acetylated histone tails (Ladurner et al. 2003). Unlike fission yeast Bdf2, budding yeast Bdf1 does not specifically localize to defined boundary elements but is recruited to the transition zone, in which a gradient of H4K16ac is formed by the actions of HAT SAS2 and HDAC Sir2 (Kimura et al. 2002; Suka et al. 2002; Ladurner et al. 2003). Bdf1 is also part of the Swr1 complex that is required for the deposition of histone variant H2A.Z (Krogan et al. 2003; Kobor et al. 2004; Mizuguchi et al. 2004), which is also involved in counteracting heterochromatin spreading (Meneghini et al. 2003). There is a Bdf1 homolog in fission yeast, which is part of the fission yeast Swr1 complex (Buchanan et al. 2009; Hou et al. 2010). However, fission yeast Bdf1 is not involved in boundary function at *IRC*s (Supplemental Fig. S14).

### *H4K16ac and heterochromatin spreading in fission yeast*

The bromodomains of Bdf2 interact with tetra-acetylated but not singly acetylated histone H4 tail peptides in vitro. This is consistent with studies of human BET family proteins, which favor multiply acetylated substrates (Filippakopoulos et al. 2012). Mutational analysis of acetylated lysines on the histone H4 tail in budding yeast demonstrates that Lys5, Lys8, Lys12, and Lys16 are partially redundant and cumulatively regulate gene expression, heterochromatin assembly, maintenance of genome integrity, and cell cycle progression, although Lys16 acetylation has a more dominant role (Megee et al. 1990, 1995;

Park and Szostak 1990; Durrin et al. 1991; Dion et al. 2005). The fact that fission yeast Sir2 preferentially deacetylates K16 among the H4 tail lysines (Shankaranarayana et al. 2003; Alper et al. 2013) and that Bdf2 counteracts Sir2 to regulate H4K16ac levels at *IRC*s suggests that acetylated H4K16 is a major target of Bdf2 in vivo. Indeed, the association of Bdf2 with *IRC*s and gene promoters is significantly reduced in *H4K16R* cells (Fig. 6F; Supplemental Fig. S6D).

H4K16ac directly regulates the compaction of nucleosomal arrays in vitro (Shogren-Knaak et al. 2006), and in budding yeast, H4K16ac is critical for regulating heterochromatin spreading in vivo (Kimura et al. 2002; Suka et al. 2002). In fission yeast, eliminating H4K16ac with a *H4K16R* mutation resulted in heterochromatin spreading outside of *IRC1R*, and mimicking hyperacetylation of H4K16 with a *H4K16Q* mutation effectively blocked heterochromatin spreading in *bdf2Δ* and *epe1Δ* cells. Such results suggest that deacetylation of H4K16 is an integral part of H3K9me and Swi6-mediated heterochromatin spreading. However, H4K16ac-mimicking mutations such as *H4K16A* and *H4K16Q* have little effect on silencing of reporter genes inserted inside pericentric repeats such as *otr::ade6*$^{+}$ (Supplemental Fig. S15; Mellone et al. 2003), indicating that additional heterochromatin assembly pathways at pericentric regions, such as RNAi, can overcome the requirement of Sir2 (Alper et al. 2013; Buscaino et al. 2013).

In both budding yeast and fission yeast, Sir2 is the conserved HDAC that regulates heterochromatin assembly (Kimura et al. 2002; Suka et al. 2002; Shankaranarayana et al. 2003; Freeman-Cook et al. 2005; Buscaino et al. 2013). In fission yeast, it was proposed that Sir2-mediated deacetylation of H3K9 is a prerequisite for H3K9me (Shankaranarayana et al. 2003). However, *sir2Δ* has only minor effects on H3K9me levels at heterochromatin nucleation centers such as pericentric repeats or the *cenH* sequence at the mating type region (Shankaranarayana et al. 2003; Freeman-Cook et al. 2005; Alper et al. 2013; Buscaino et al. 2013), suggesting that deacetylation of H3K9 in the absence of Sir2 can be accomplished by other HDACs. Our results that Sir2 regulates H4K16ac levels at heterochromatin boundaries and that H4K16 mutants modulate heterochromatin boundary function suggest that Sir2 also deacetylates H4K16 in regulating heterochromatin spreading. We hypothesize that the deacetylation of H4K16 increases chromatin compaction levels, thus bringing the adjacent nucleosomes closer to Clr4 for repeated cycles of H3K9me propagation. The fact that reducing histone dosage affects the ability of heterochromatin to spread (Supplemental Fig. S10) also supports such a hypothesis.

In budding yeast, Sas2 is the major H4K16 acetyltransferase that regulates silencing and boundary formation (Kimura et al. 2002; Suka et al. 2002; Shia et al. 2006). However, there is no Sas2 homolog in fission yeast. We discovered that the fission yeast MYST family acetyltransferase Mst1 is required for H4K16ac and the binding of Bdf2 at *IRC*s, and a mutation in Mst1 also resulted in defects in boundary formation at *IRC*s. Mst1 forms a complex with composition similar to that of the budding yeast NuA4, which acetylates H4K16 as well as other residues (Lee and Workman 2007; Gomez et al. 2008; Shevchenko et al. 2008). However, in budding yeast, mutations in Esa1, the catalytic subunit of NuA4, have no effect on telomeric heterochromatin assembly (Kimura et al. 2002; Suka et al. 2002). Thus, the fission yeast Mst1 complex has taken over the role of both Sas2 and NuA4 complexes in budding yeast, which might be attributed to the slight difference in the composition of Mst1 and NuA4 complexes (Shevchenko et al. 2008).

### *Overexpression of Swi6 enhances heterochromatin spreading*

Multiple mechanisms cooperate to establish heterochromatin boundaries. In addition to Epe1, TFIIIC binding to *IR* elements contributes to boundary formation at the silent mating type region, and tRNA genes and transcription of *IRC1* contribute to boundary activity at centromeres (Noma et al. 2006; Scott et al. 2006; Keller et al. 2013). As a result, heterochromatin spreading in *epe1Δ* cells is a stochastic event happening only in a small portion of cells. Although the reporter-based assays provide sensitive readouts of heterochromatin spreading in this subpopulation, it is difficult to perform biochemical assays with ensembles of cells, since the majority of cells do not show spreading. For example, our ChIP–chip analysis showed that in *epe1Δ* cells without Swi6 overexpression or reporter-based selection, H3K9me2 levels around *IRC1* were similar to those of wild-type cells (data not shown), consistent with earlier analysis of H3K9me2 levels in *epe1Δ* cells at the mating type region and centromeres (Ayoub et al. 2003; Braun et al. 2011). The use of an additional copy of Swi6 provides a more profound effect on heterochromatin spreading at centromere boundaries, and similar approaches have been used to enhance heterochromatin spreading at the mating type region (Noma et al. 2001, 2006).

### *The functions of Bdf2 in other processes*

In addition to its role in boundary function, Bdf2 also interacted with a number of TAFs, and our ChIP–chip analysis showed that Bdf2 localized at a small group of gene promoters (~13% of all promoter probes in our microarray), suggesting that Bdf2 might be involved in transcriptional regulation of certain genes. *IRC*s were transcribed (Zofall and Grewal 2006; Keller et al. 2013), and *IRC1* transcript levels were strongly reduced in *bdf2Δ* and *epe1Δ* cells (Supplemental Fig. S16), suggesting that Bdf2 regulates transcription of *IRC*s. However, targeting of Bdf2 to Gal4-binding sites is sufficient to block the spreading of heterochromatin at an ectopic site in a bromodomain-dependent manner, suggesting that the ability of Bdf2 to counteract heterochromatin spreading is through protection of H4K16ac by its bromodomains, although transcription of *IRC*s has an independent contribution to boundary function (Keller et al. 2013). It is also possible that Bdf2 regulates transcription of other factors involved in heterochromatin boundary functions, and it would be interesting to determine the role of Bdf2

in regulating gene expression at euchromatic regions in the future. Bdf2 has also been shown to regulate DNA damage response, which is attributed to its effect on regulating global H4 acetylation levels (Garabedian et al. 2012).

### *Implications of BET protein functions in other systems*

The BET family of bromodomains in mammals includes BRD2, BRD3, BRD4, and BRDT. They associate with diverse protein complexes involved in chromatin modifications and play important roles in transcription regulation, cell cycle control, gene bookmarking, and viral genome transcription (Belkina and Denis 2012). Misregulation of BET proteins, especially Brd4, has been linked to a number of human cancers. For example, chromosome translocation between BRD4 and NUT (nuclear protein in testis) leads to a highly lethal form of carcinoma, and BRD4 is a therapeutic target in acute myeloid leukemia (French et al. 2003; Zuber et al. 2011). The identification of small molecules such as JQ1 and IBET that inhibit the binding of BET family bromodomains to chromatin (Filippakopoulos et al. 2010; Nicodeme et al. 2010) makes them the focus of drug-mediated epigenetic treatment of diverse types of cancers (Dawson et al. 2011; Delmore et al. 2011; Mertz et al. 2011; Zuber et al. 2011; Loven et al. 2013). Although the precise mechanism of these inhibitors is not well understood, the displacement of BET proteins from chromatin in part down-regulates oncogene c-Myc to promote differentiation (Dawson et al. 2011; Mertz et al. 2011; Zuber et al. 2011; Loven et al. 2013). However, mice treated with these drugs do not exhibit tissue-renewing defects associated with lower Myc activity, indicative of additional mechanisms (Filippakopoulos et al. 2010; Dawson et al. 2011; Delmore et al. 2011; Mertz et al. 2011; Zuber et al. 2011). The fact that BET domain proteins Bdf2 in fission yeast and Bdf1 in budding yeast regulate heterochromatin spreading suggests that BET inhibitors may affect the spreading of heterochromatin and reset the epigenetic landscape in cancer cells. In other multicellular organisms such as zebrafish, worms, and flies, BET proteins are essential for the determination of cell fate during development (Huang and Dawid 1990; Chang et al. 2007; Dibenedetto et al. 2008; Shibata et al. 2010). In particular, the *Drosophila* BET protein FSH (female sterile 1 homeotic) is classified as a Trithorax group gene that counteracts Polycomb group protein-mediated gene silencing (Chang et al. 2007; Kockmann et al. 2013). Thus, it seems that the function of BET proteins in antagonizing gene silencing is highly conserved across species.

## Materials and methods

### *Fission yeast strains and genetic analyses*

The *IRC1R::ura4*$^+$ reporter was constructed by inserting *ura4*$^+$ at the right side of *IRC1R* (chromosome I, 3790595). The query strain used for our screen contains a closely linked *natMX6* cassette (chromosome I, 3804996). *IRC1RΔ* removed chromosome I: 3789581–3790711. The *IRC3L::ura4*$^+$ reporter was constructed by inserting *ura4*$^+$ at the left side of *IRC3L* (chromosome III, 1067955). *L5-IRC1R-ura4*$^+$ and *L5-3gbs-ura4*$^+$ strains were constructed by inserting *IRC1R* or *3gbs* sequences between *L5* and *ura4*$^+$ using *L5-ura4*$^+$ (Sadaie et al. 2004) as a template. Bdf2-Flag, Bdf2-myc, and Epe1-Flag were constructed by a PCR-based module method. *bdf2Δ*, *epe1Δ*, and *sir2Δ* were derived from the Bioneer fission yeast deletion library, verified via PCR, and backcrossed. The *bdf2-ΔC* and *bdf2-2YA* strains were constructed by integrating a PCR fragment containing the mutations and a *Flag-kanMX6* cassette into the endogenous *bdf2*$^+$ locus. *H4K16R* and *H4K16Q* mutations were constructed and introduced into the *h4.1Δ/h4.3Δ* background as described previously (Mellone et al. 2003), with the exception of introducing a linked *natMX6* cassette. Genetic crosses were used to construct all other strains. For serial dilution plating assays, 10-fold dilutions of a log-phase culture were plated on the indicated medium and grown for 3 d at 30°C. All strains used in heterochromatin spreading assays contain an extra copy of the *swi6*$^+$ gene inserted at the *ade6* locus and driven by the *ade6* promoter to enhance heterochromatin spreading. A list of the yeast strains used is provided in Supplemental Table S3.

### *ChIP analysis*

ChIP analyses were performed as described previously (Hou et al. 2010). Antibodies used were H3K9me2 (Abcam, ab1220), H4K16ac (Active Motif, 39167), H3 (Abcam, ab1791), H4 (Abcam, ab10158), and Flag (Sigma, A2220). Swi6 antibody was custom-made with full-length recombinant Swi6 protein and affinity-purified (Reddy et al. 2011).

ChIP–chip analysis was performed according to the Agilent Yeast ChIP-on-chip Analysis protocol. The microarray used was an Agilent *Schizosaccharomyces pombe* Whole-Genome ChIP-on-chip microarray (G4810A) with additional probes that encompass centromeres, which were originally absent from the array due to the repetitive nature of these DNA sequences. Blunt-end DNA was generated from immunoprecipitated chromatin fractions (ChIP) or whole-cell extract (WCE) with T4 DNA polymerase and then ligated to a linker. ChIP and WCE DNA were amplified from blunt-end DNA samples with primers annealing to the linker and were labeled by Cy5-dUTP or Cy3-dUTP, respectively, with random priming PCR (Invitrogen CGH kit). Three micrograms of Cy5-labeled ChIP DNA and the corresponding Cy3-labled WCE DNA were hybridized to the microarray. The slides were washed and processed in accordance with Agilent protocols and scanned with an Agilent scanner. Data were collected with the Agilent Feature Extraction program. The enrichment value for each probe was calculated by dividing normalized ChIP signal by WCE signal. The data presented are averages of two independent ChIP–chip experiments. ChIP–chip data have been submitted to the Gene Expression Omnibus under accession number GSE46430.

qPCR was performed with Maxima SYBR Green qPCR Master Mix (Thermo Scientific) in a StepOne Plus Real-Time PCR System (Applied Biosystems). DNA serial dilutions were used as templates to generate a standard curve of amplification for each pair of primers, and the relative concentrations of target sequence and a control *act1* sequence in ChIP and WCE samples were calculated accordingly. The final enrichment was calculated as [(ChIP target)/(WCE target)]/[(ChIP *act1*)/(WCE *act1*)]. A list of the primers used is provided in Supplemental Table S4.

### *Protein purification, coimmunoprecipitation, and mass spectrometry analysis*

Exponentially growing yeast cells were harvested, washed with 2× HC buffer (300 mM HEPES-KOH at pH 7.6, 2 mM EDTA, 100 mM KCl, 20% glycerol, 2 mM DTT, protease inhibitor

cocktail [Roche]), and frozen in liquid nitrogen. Crude cell extracts were prepared by vigorously blending frozen yeast cells with dry ice using a household blender, followed by incubation with 30 mL of 1× HC buffer containing 250 mM KCl for 30 min. The lysate was cleared by centrifugation at 82,700*g* for 3 h. The supernatants were precleared with protein A agarose, then incubated with 200 μL of Flag-agarose overnight, and washed eight times with 1× HC containing 250 mM KCl. For mass spectrometry analysis, bound proteins were eluted with 200 μg/mL 3xFlag peptides followed by TCA precipitation. Multidimensional protein identification technology (MudPIT) mass spectrometry analysis was performed as described previously (Wang et al. 2009). For coimmunoprecipitation analysis, bound proteins were resolved by SDS-PAGE followed by Western blot analyses with Myc (Santa Cruz Biotechnology, sc-789) and Flag (Sigma, F7425) antibodies.

### *Peptide-binding assays*

The bromodomains of Bdf2 (amino acids 229–497) were cloned into pGEX or pRSET bacterial expression vector. The 2YA mutant was generated by site-directed mutagenesis according to the manufacturer's protocol (Agilent). Recombinant GST and His-tagged Bdf2 proteins were purified with Glutathione Sepharose 4B (GE) and Talon Metal Affinity Resin (Clontech), respectively, according to manufacturer's protocols, followed by gel filtration with a Superdex 200 column. Binding of GST-Bdf2-BD to a Modified Histone Peptide Array (Active Motif, catalog no. 17-0756-01) was performed according to the manufacturer's protocol. The array contains 59 different post-translational modifications for histone acetylation, methylation, phosphorylation, and citrullination on the N-terminal tails of histones H2A, H2B, H3, and H4 (Supplemental Table S2). Each 19mer peptide may contain up to four modifications. Array Analyze software (Active Motif) was used to analyze spot intensity from the image. The results were graphed as a specificity factor, which is the ratio of the average intensity of all spots containing the mark divided by the average intensity of all spots not containing the mark. For peptide pull-down assays, 1 μg of recombinant proteins was incubated with 1 μg of biotinylated H3 or H4 histone peptides (Millipore, catalog nos. 12-403 for H3, 12-402 for Ac-H3, 12-372 for H4, and 12-379 for Ac-H4) in 1× HC buffer containing 200 mM KCl overnight at 4°C and washed extensively. Bound fractions were resolved by SDS-PAGE and visualized by silver staining.

### *Yeast two-hybrid assay*

Full-length Bdf2, Bdf2-ΔN, Bdf2-ΔC, and Bdf2-BD were cloned into the XmaI/BamHI site of pGBT9 (Clontech) to generate fusion with the GAL4 DNA-binding domain. Epe1 was cloned into the PstI/BglII site of pGAD424 (Clontech) to generate fusion with the GAL4 activation domain. Both plasmids were transformed into the budding yeast strain pJ69-4A, and transformants were selected on medium lacking tryptophan and leucine to maintain both plasmids. The interaction of the two proteins was indicated by the activation of a *HIS3* reporter, allowing growth on medium lacking histidine.

### *RNA extraction and RT–PCR*

Total cellular RNA was isolated from log-phase cells using MasterPure yeast RNA purification kit (Epicentre) according to the manufacturer's protocol. Quantification with real-time RT–PCR was performed with Power SYBR Green RNA-to-CT one-step kit (Applied Biosystems). RNA serial dilutions were used as a template to generate a standard curve of amplification for each pair of primers, and the relative concentration of the target sequence was calculated accordingly. An *act1* fragment served as a reference to normalize the concentration of samples. The concentration of each target gene in wild type was arbitrarily set to 1 and served as a reference for other samples.

### *Sir2 HDAC assay*

Full-length Sir2 cDNA was cloned into the pRSET bacterial expression vector (Invitrogen). Recombinant His-tagged Sir2 protein was purified with Talon Metal Affinity Resin (Clontech) according to the manufacturer's protocol. Sir2 HDAC assay was performed using the SIRTainty Class III HDAC assay kit (Millipore) according to the manufacturer's protocol. Briefly, 5 μg of recombinant Bdf2 or Bdf2-2YA proteins was incubated with β-NAD, nicotinamidase, tetra-acetylated H4 peptides, and different amounts of recombinant Sir2 for 1 h at 37°C followed by further incubation with developer reagent for 1 h at room temperature. Fluorescence intensity was measured with a BioTek Synergy 4 Hybrid Microplate Reader with filter set to excitation at 420 nm and emission at 470 nm.

## Acknowledgments

We thank Anudari Letian for technical assistance; Robin Allshire, Amar Klar, Jun-ichi Nakayama, Janet Partridge, and the National BioResource project in Japan for yeast strains; Michael Keogh for communicating unpublished results; and James Manley, Scott Kallgren, Allison Cohen, and Eric Wei for critical reading of the manuscript. This work is supported by National Institutes of Health grants R01-GM085145 to S.J., the National Center for Research Resources (P41-RR011823), and National Institute of General Medical Sciences (P41-GM103533). X.T. is a Fulbright Scholar.

## References

Alper BJ, Job G, Yadav RK, Shanker S, Lowe BR, Partridge JF. 2013. Sir2 is required for Clr4 to initiate centromeric heterochromatin assembly in fission yeast. *EMBO J* doi: 10.1038/emboj.2013.143.

Ayoub N, Noma K, Isaac S, Kahan T, Grewal SI, Cohen A. 2003. A novel jmjC domain protein modulates heterochromatization in fission yeast. *Mol Cell Biol* **23:** 4356–4370.

Bannister AJ, Kouzarides T. 2011. Regulation of chromatin by histone modifications. *Cell Res* **21:** 381–395.

Bannister AJ, Zegerman P, Partridge JF, Miska EA, Thomas JO, Allshire RC, Kouzarides T. 2001. Selective recognition of methylated lysine 9 on histone H3 by the HP1 chromo domain. *Nature* **410:** 120–124.

Beisel C, Paro R. 2011. Silencing chromatin: Comparing modes and mechanisms. *Nat Rev Genet* **12:** 123–135.

Belkina AC, Denis GV. 2012. BET domain co-regulators in obesity, inflammation and cancer. *Nat Rev Cancer* **12:** 465–477.

Braun S, Garcia JF, Rowley M, Rougemaille M, Shankar S, Madhani HD. 2011. The Cul4–Ddb1(Cdt)(2) ubiquitin ligase inhibits invasion of a boundary-associated antisilencing factor into heterochromatin. *Cell* **144:** 41–54.

Buchanan L, Durand-Dubief M, Roguev A, Sakalar C, Wilhelm B, Stralfors A, Shevchenko A, Aasland R, Ekwall K, Francis Stewart A. 2009. The *Schizosaccharomyces pombe* JmjC-protein, Msc1, prevents H2A.Z localization in centromeric and subtelomeric chromatin domains. *PLoS Genet* **5:** e1000726.

Buscaino A, Lejeune E, Audergon P, Hamilton G, Pidoux A, Allshire RC. 2013. Distinct roles for Sir2 and RNAi in

centromeric heterochromatin nucleation, spreading and maintenance. *EMBO J* **32:** 1250–1264.
Cam HP, Sugiyama T, Chen ES, Chen X, FitzGerald PC, Grewal SI. 2005. Comprehensive analysis of heterochromatin- and RNAi-mediated epigenetic control of the fission yeast genome. *Nat Genet* **37:** 809–819.
Castel SE, Martienssen RA. 2013. RNA interference in the nucleus: Roles for small RNAs in transcription, epigenetics and beyond. *Nat Rev Genet* **14:** 100–112.
Chang YL, King B, Lin SC, Kennison JA, Huang DH. 2007. A double-bromodomain protein, FSH-S, activates the homeotic gene ultrabithorax through a critical promoter-proximal region. *Mol Cell Biol* **27:** 5486–5498.
Dawson MA, Prinjha RK, Dittmann A, Giotopoulos G, Bantscheff M, Chan WI, Robson SC, Chung CW, Hopf C, Savitski MM, et al. 2011. Inhibition of BET recruitment to chromatin as an effective treatment for MLL-fusion leukaemia. *Nature* **478:** 529–533.
Delmore JE, Issa GC, Lemieux ME, Rahl PB, Shi J, Jacobs HM, Kastritis E, Gilpatrick T, Paranal RM, Qi J, et al. 2011. BET bromodomain inhibition as a therapeutic strategy to target c-Myc. *Cell* **146:** 904–917.
Dibenedetto AJ, Guinto JB, Ebert TD, Bee KJ, Schmidt MM, Jackman TR. 2008. Zebrafish brd2a and brd2b are paralogous members of the bromodomain-ET (BET) family of transcriptional coregulators that show structural and expression divergence. *BMC Dev Biol* **8:** 39.
Dion MF, Altschuler SJ, Wu LF, Rando OJ. 2005. Genomic characterization reveals a simple histone H4 acetylation code. *Proc Natl Acad Sci* **102:** 5501–5506.
Durrin LK, Mann RK, Kayne PS, Grunstein M. 1991. Yeast histone H4 N-terminal sequence is required for promoter activation in vivo. *Cell* **65:** 1023–1031.
Elgin SC, Reuter G. 2007. Position-effect variegation, heterochromatin formation, and gene silencing in *Drosophila*. In *Epigenetics* (ed. Allis CD, et al.), pp. 81–100. Cold Spring Harbor Laboratory Press, Cold Spring Harbor, NY.
Filippakopoulos P, Qi J, Picaud S, Shen Y, Smith WB, Fedorov O, Morse EM, Keates T, Hickman TT, Felletar I, et al. 2010. Selective inhibition of BET bromodomains. *Nature* **468:** 1067–1073.
Filippakopoulos P, Picaud S, Mangos M, Keates T, Lambert JP, Barsyte-Lovejoy D, Felletar I, Volkmer R, Muller S, Pawson T, et al. 2012. Histone recognition and large-scale structural analysis of the human bromodomain family. *Cell* **149:** 214–231.
Freeman-Cook LL, Gomez EB, Spedale EJ, Marlett J, Forsburg SL, Pillus L, Laurenson P. 2005. Conserved locus-specific silencing functions of *Schizosaccharomyces pombe* sir2$^+$. *Genetics* **169:** 1243–1260.
French CA, Miyoshi I, Kubonishi I, Grier HE, Perez-Atayde AR, Fletcher JA. 2003. BRD4–NUT fusion oncogene: A novel mechanism in aggressive carcinoma. *Cancer Res* **63:** 304–307.
Garabedian MV, Noguchi C, Ziegler MA, Das MM, Singh T, Harper LJ, Leman AR, Khair L, Moser BA, Nakamura TM, et al. 2012. The double-bromodomain proteins Bdf1 and Bdf2 modulate chromatin structure to regulate S-phase stress response in *Schizosaccharomyces pombe*. *Genetics* **190:** 487–500.
Gaszner M, Felsenfeld G. 2006. Insulators: Exploiting transcriptional and epigenetic mechanisms. *Nat Rev Genet* **7:** 703–713.
Gomez EB, Espinosa JM, Forsburg SL. 2005. *Schizosaccharomyces pombe* mst2+ encodes a MYST family histone acetyltransferase that negatively regulates telomere silencing. *Mol Cell Biol* **25:** 8887–8903.
Gomez EB, Nugent RL, Laria S, Forsburg SL. 2008. *Schizosaccharomyces pombe* histone acetyltransferase Mst1 (KAT5) is an essential protein required for damage response and chromosome segregation. *Genetics* **179:** 757–771.
Grewal SI, Elgin SC. 2007. Transcription and RNA interference in the formation of heterochromatin. *Nature* **447:** 399–406.
Grewal SI, Jia S. 2007. Heterochromatin revisited. *Nat Rev Genet* **8:** 35–46.
Hall IM, Shankaranarayana GD, Noma K, Ayoub N, Cohen A, Grewal SI. 2002. Establishment and maintenance of a heterochromatin domain. *Science* **297:** 2232–2237.
Hong EJ, Villen J, Gerace EL, Gygi SP, Moazed D. 2005. A cullin E3 ubiquitin ligase complex associates with Rik1 and the Clr4 histone H3-K9 methyltransferase and is required for RNAi-mediated heterochromatin formation. *RNA Biol* **2:** 106–111.
Horn PJ, Bastie JN, Peterson CL. 2005. A Rik1-associated, cullin-dependent E3 ubiquitin ligase is essential for heterochromatin formation. *Genes Dev* **19:** 1705–1714.
Hou H, Wang Y, Kallgren SP, Thompson J, Yates JR 3rd, Jia S. 2010. Histone variant H2A.Z regulates centromere silencing and chromosome segregation in fission yeast. *J Biol Chem* **285:** 1909–1918.
Huang DH, Dawid IB. 1990. The maternal-effect gene fsh is essential for the specification of the central region of the *Drosophila* embryo. *New Biol* **2:** 163–170.
Ishii K, Arib G, Lin C, Van Houwe G, Laemmli UK. 2002. Chromatin boundaries in budding yeast: The nuclear pore connection. *Cell* **109:** 551–562.
Jia S, Noma K, Grewal SI. 2004. RNAi-independent heterochromatin nucleation by the stress-activated ATF/CREB family proteins. *Science* **304:** 1971–1976.
Jia S, Kobayashi R, Grewal SI. 2005. Ubiquitin ligase component Cul4 associates with Clr4 histone methyltransferase to assemble heterochromatin. *Nat Cell Biol* **7:** 1007–1013.
Kanoh J, Sadaie M, Urano T, Ishikawa F. 2005. Telomere binding protein Taz1 establishes Swi6 heterochromatin independently of RNAi at telomeres. *Curr Biol* **15:** 1808–1819.
Keller C, Kulasegaran-Shylini R, Shimada Y, Hotz HR, Buhler M. 2013. Noncoding RNAs prevent spreading of a repressive histone mark. *Nat Struct Mol Biol* **20:** 994–1000.
Kim DU, Hayles J, Kim D, Wood V, Park HO, Won M, Yoo HS, Duhig T, Nam M, Palmer G, et al. 2010. Analysis of a genome-wide set of gene deletions in the fission yeast *Schizosaccharomyces pombe*. *Nat Biotechnol* **28:** 617–623.
Kimura A, Horikoshi M. 2004. Partition of distinct chromosomal regions: Negotiable border and fixed border. *Genes Cells* **9:** 499–508.
Kimura A, Umehara T, Horikoshi M. 2002. Chromosomal gradient of histone acetylation established by Sas2p and Sir2p functions as a shield against gene silencing. *Nat Genet* **32:** 370–377.
Kobor MS, Venkatasubrahmanyam S, Meneghini MD, Gin JW, Jennings JL, Link AJ, Madhani HD, Rine J. 2004. A protein complex containing the conserved Swi2/Snf2-related ATPase Swr1p deposits histone variant H2A.Z into euchromatin. *PLoS Biol* **2:** E131.
Kockmann T, Gerstung M, Schlumpf T, Xhinzhou Z, Hess D, Beerenwinkel N, Beisel C, Paro R. 2013. The BET protein FSH functionally interacts with ASH1 to orchestrate global gene activity in *Drosophila*. *Genome Biol* **14:** R18.
Krogan NJ, Keogh MC, Datta N, Sawa C, Ryan OW, Ding H, Haw RA, Pootoolal J, Tong A, Canadien V, et al. 2003. A Snf2 family ATPase complex required for recruitment of the histone H2A variant Htz1. *Mol Cell* **12:** 1565–1576.
Kurdistani SK, Grunstein M. 2003. Histone acetylation and deacetylation in yeast. *Nat Rev Mol Cell Biol* **4:** 276–284.

Ladurner AG, Inouye C, Jain R, Tjian R. 2003. Bromodomains mediate an acetyl-histone encoded antisilencing function at heterochromatin boundaries. *Mol Cell* **11:** 365–376.

Lee KK, Workman JL. 2007. Histone acetyltransferase complexes: One size doesn't fit all. *Nat Rev Mol Cell Biol* **8:** 284–295.

Lejeune E, Allshire RC. 2011. Common ground: Small RNA programming and chromatin modifications. *Curr Opin Cell Biol* **23:** 258–265.

Loven J, Hoke HA, Lin CY, Lau A, Orlando DA, Vakoc CR, Bradner JE, Lee TI, Young RA. 2013. Selective inhibition of tumor oncogenes by disruption of super-enhancers. *Cell* **153:** 320–334.

Megee PC, Morgan BA, Mittman BA, Smith MM. 1990. Genetic analysis of histone H4: Essential role of lysines subject to reversible acetylation. *Science* **247:** 841–845.

Megee PC, Morgan BA, Smith MM. 1995. Histone H4 and the maintenance of genome integrity. *Genes Dev* **9:** 1716–1727.

Mellone BG, Ball L, Suka N, Grunstein MR, Partridge JF, Allshire RC. 2003. Centromere silencing and function in fission yeast is governed by the amino terminus of histone H3. *Curr Biol* **13:** 1748–1757.

Meneghini MD, Wu M, Madhani HD. 2003. Conserved histone variant H2A.Z protects euchromatin from the ectopic spread of silent heterochromatin. *Cell* **112:** 725–736.

Mertz JA, Conery AR, Bryant BM, Sandy P, Balasubramanian S, Mele DA, Bergeron L, Sims RJ 3rd. 2011. Targeting MYC dependence in cancer by inhibiting BET bromodomains. *Proc Natl Acad Sci* **108:** 16669–16674.

Mizuguchi G, Shen X, Landry J, Wu WH, Sen S, Wu C. 2004. ATP-driven exchange of histone H2AZ variant catalyzed by SWR1 chromatin remodeling complex. *Science* **303:** 343–348.

Moazed D. 2009. Small RNAs in transcriptional gene silencing and genome defence. *Nature* **457:** 413–420.

Moazed D. 2011. Mechanisms for the inheritance of chromatin states. *Cell* **146:** 510–518.

Mujtaba S, Zeng L, Zhou MM. 2007. Structure and acetyl-lysine recognition of the bromodomain. *Oncogene* **26:** 5521–5527.

Nakayama J, Rice JC, Strahl BD, Allis CD, Grewal SI. 2001. Role of histone H3 lysine 9 methylation in epigenetic control of heterochromatin assembly. *Science* **292:** 110–113.

Nicodeme E, Jeffrey KL, Schaefer U, Beinke S, Dewell S, Chung CW, Chandwani R, Marazzi I, Wilson P, Coste H, et al. 2010. Suppression of inflammation by a synthetic histone mimic. *Nature* **468:** 1119–1123.

Noma K, Allis CD, Grewal SI. 2001. Transitions in distinct histone H3 methylation patterns at the heterochromatin domain boundaries. *Science* **293:** 1150–1155.

Noma K, Cam HP, Maraia RJ, Grewal SI. 2006. A role for TFIIIC transcription factor complex in genome organization. *Cell* **125:** 859–872.

Oki M, Valenzuela L, Chiba T, Ito T, Kamakaka RT. 2004. Barrier proteins remodel and modify chromatin to restrict silenced domains. *Mol Cell Biol* **24:** 1956–1967.

Park EC, Szostak JW. 1990. Point mutations in the yeast histone H4 gene prevent silencing of the silent mating type locus HML. *Mol Cell Biol* **10:** 4932–4934.

Partridge JF, Scott KS, Bannister AJ, Kouzarides T, Allshire RC. 2002. *cis*-acting DNA from fission yeast centromeres mediates histone H3 methylation and recruitment of silencing factors and cohesin to an ectopic site. *Curr Biol* **12:** 1652–1660.

Paule MR, White RJ. 2000. Survey and summary: Transcription by RNA polymerases I and III. *Nucleic Acids Res* **28:** 1283–1298.

Prinjha RK, Witherington J, Lee K. 2012. Place your BETs: The therapeutic potential of bromodomains. *Trends Pharmacol Sci* **33:** 146–153.

Rea S, Eisenhaber F, O'Carroll D, Strahl BD, Sun ZW, Schmid M, Opravil S, Mechtler K, Ponting CP, Allis CD, et al. 2000. Regulation of chromatin structure by site-specific histone H3 methyltransferases. *Nature* **406:** 593–599.

Reddy BD, Wang Y, Niu L, Higuchi EC, Marguerat SB, Bahler J, Smith GR, Jia S. 2011. Elimination of a specific histone H3K14 acetyltransferase complex bypasses the RNAi pathway to regulate pericentric heterochromatin functions. *Genes Dev* **25:** 214–219.

Rusche LN, Kirchmaier AL, Rine J. 2003. The establishment, inheritance, and function of silenced chromatin in *Saccharomyces cerevisiae*. *Annu Rev Biochem* **72:** 481–516.

Sadaie M, Iida T, Urano T, Nakayama J. 2004. A chromodomain protein, Chp1, is required for the establishment of heterochromatin in fission yeast. *EMBO J* **23:** 3825–3835.

Sadaie M, Kawaguchi R, Ohtani Y, Arisaka F, Tanaka K, Shirahige K, Nakayama J. 2008. Balance between distinct HP1 family proteins controls heterochromatin assembly in fission yeast. *Mol Cell Biol* **28:** 6973–6988.

Schotta G, Ebert A, Krauss V, Fischer A, Hoffmann J, Rea S, Jenuwein T, Dorn R, Reuter G. 2002. Central role of *Drosophila* SU(VAR)3-9 in histone H3-K9 methylation and heterochromatic gene silencing. *EMBO J* **21:** 1121–1131.

Scott KC, Merrett SL, Willard HF. 2006. A heterochromatin barrier partitions the fission yeast centromere into discrete chromatin domains. *Curr Biol* **16:** 119–129.

Shankaranarayana GD, Motamedi MR, Moazed D, Grewal SI. 2003. Sir2 regulates histone H3 lysine 9 methylation and heterochromatin assembly in fission yeast. *Curr Biol* **13:** 1240–1246.

Shevchenko A, Roguev A, Schaft D, Buchanan L, Habermann B, Sakalar C, Thomas H, Krogan NJ, Stewart AF. 2008. Chromatin central: Towards the comparative proteome by accurate mapping of the yeast proteomic environment. *Genome Biol* **9:** R167.

Shia WJ, Li B, Workman JL. 2006. SAS-mediated acetylation of histone H4 Lys 16 is required for H2A.Z incorporation at subtelomeric regions in *Saccharomyces cerevisiae*. *Genes Dev* **20:** 2507–2512.

Shibata Y, Takeshita H, Sasakawa N, Sawa H. 2010. Double bromodomain protein BET-1 and MYST HATs establish and maintain stable cell fates in *C. elegans*. *Development* **137:** 1045–1053.

Shogren-Knaak M, Ishii H, Sun JM, Pazin MJ, Davie JR, Peterson CL. 2006. Histone H4-K16 acetylation controls chromatin structure and protein interactions. *Science* **311:** 844–847.

Singh G, Klar AJ. 2008. Mutations in deoxyribonucleotide biosynthesis pathway cause spreading of silencing across heterochromatic barriers at the mating-type region of the fission yeast. *Yeast* **25:** 117–128.

Stewart MD, Li J, Wong J. 2005. Relationship between histone H3 lysine 9 methylation, transcription repression, and heterochromatin protein 1 recruitment. *Mol Cell Biol* **25:** 2525–2538.

Suka N, Luo K, Grunstein M. 2002. Sir2p and Sas2p opposingly regulate acetylation of yeast histone H4 lysine16 and spreading of heterochromatin. *Nat Genet* **32:** 378–383.

Talbert PB, Henikoff S. 2006. Spreading of silent chromatin: Inaction at a distance. *Nat Rev Genet* **7:** 793–803.

Trewick SC, McLaughlin PJ, Allshire RC. 2005. Methylation: Lost in hydroxylation? *EMBO Rep* **6:** 315–320.

Trewick SC, Minc E, Antonelli R, Urano T, Allshire RC. 2007. The JmjC domain protein Epe1 prevents unregulated

assembly and disassembly of heterochromatin. *EMBO J* **26:** 4670–4682.
Tsukada Y, Fang J, Erdjument-Bromage H, Warren ME, Borchers CH, Tempst P, Zhang Y. 2006. Histone demethylation by a family of JmjC domain-containing proteins. *Nature* **439:** 811–816.
Valenzuela L, Kamakaka RT. 2006. Chromatin insulators. *Annu Rev Genet* **40:** 107–138.
Wang Y, Reddy B, Thompson J, Wang H, Noma K, Yates JR 3rd, Jia S. 2009. Regulation of Set9-mediated H4K20 methylation by a PWWP domain protein. *Mol Cell* **33:** 428–437.
West AG, Huang S, Gaszner M, Litt MD, Felsenfeld G. 2004. Recruitment of histone modifications by USF proteins at a vertebrate barrier element. *Mol Cell* **16:** 453–463.
Zentner GE, Henikoff S. 2013. Regulation of nucleosome dynamics by histone modifications. *Nat Struct Mol Biol* **20:** 259–266.
Zhang K, Mosch K, Fischle W, Grewal SI. 2008. Roles of the Clr4 methyltransferase complex in nucleation, spreading and maintenance of heterochromatin. *Nat Struct Mol Biol* **15:** 381–388.
Zofall M, Grewal SI. 2006. Swi6/HP1 recruits a JmjC domain protein to facilitate transcription of heterochromatic repeats. *Mol Cell* **22:** 681–692.
Zuber J, Shi J, Wang E, Rappaport AR, Herrmann H, Sison EA, Magoon D, Qi J, Blatt K, Wunderlich M, et al. 2011. RNAi screen identifies Brd4 as a therapeutic target in acute myeloid leukaemia. *Nature* **478:** 524–528.